Final version published as Fernandez-Alvarez V. M.; Eikerling M. H., ACS Appl. Mater. Interfaces 2019. DOI: 10.1021/acsami.9b16326

Interface properties of the partially oxidized Pt(111) surface using hybrid DFT-solvation models

Victor M. Fernandez-Alvarez[1] *and Michael H. Eikerling*[1,2]

Keywords: *ab initio* simulations, hybrid DFT methods, electrocatalysis, oxygen reduction reaction, electrochemical interface, metal charging relation.

Abstract

This article reports a theoretical-computational effort to model the interface between an oxidized platinum surface and aqueous electrolyte. It strives to account for the impact of the electrode potential, the formation of surface-bound oxygen species, orientational ordering of near-surface solvent molecules, and metal surface charging on the potential profile along the normal direction. The computational scheme is based on the DFT/ESM-RISM method to simulate the charged Pt(111) surface with varying number of oxygen adatoms in acidic solution. This hybrid solvation method is known to qualitatively reproduce bulk metal properties like the work function. However, the presented calculations reveal that vital interface properties such as the electrostatic potential at the outer Helmholtz plane are highly sensitive to the position of the metal surface slab relative to the DFT-RISM boundary region. Shifting the relative position of the slab also affects the free energy of the system. It follows that there is an optimal distance for the first solvent layer within the ESM-RISM framework which could be found by optimizing the position of the frozen Pt(111)

slab. As it stands, manual sampling of the position of the slab is impractical and betrays the self-consistency of the method. Based on this understanding, we propose the implementation of a free energy optimization scheme of the relative position of the slab in the DFT-RISM boundary region. This optimization scheme could considerably increase the applicability of the hybrid method.

[1] Department of Chemistry, Simon Fraser University, 8888 University Drive, Burnaby, BC V5A 1S6, Canada

[2] New affiliation: Forschungszentrum Jülich, Institute of Energy and Climate Research - Modeling and Simulation of Materials in Energy Technology (IEK-13), 52425 Jülich, Germany

INTRODUCTION

The interfacial region between a metal electrode and a liquid electrolyte lies at the heart of a multitude of technologies for energy storage and conversion.[1,2] Understanding the properties of this region, also referred to as the electrochemical double layer (EDL), has driven extensive research forays in electrochemistry.[3,4,5] Despite these efforts, crucial aspects of the EDL remain poorly understood and controversial.[6,7] Obtaining accurate information on microscopic structural details under realistic conditions remains beyond the capabilities of experimental exploration. The challenge to understand atomic scale phenomena taking place in the boundary region brings into focus theoretical models and computational studies.[8,9,10,11,12,13]

Atomic scale information on electronic and nuclear structure of solids can be reliably obtained using *ab initio* methods like density functional theory (DFT).[14] Yet there are still two main challenges hindering a predictive and transferrable theoretical description of the EDL. One is the atomic scale description of the electrostatic interactions between the liquid electrolyte and the solid metal surface. While some attempts have been made to model solid-liquid interfaces using *ab initio* molecular dynamics (AIMD),[15] most systems of interest are computationally prohibitive for such simulations. To overcome this limitation, several methods incorporate a spatially averaged continuum description of solvent interactions, which limits the structural information included. The other challenge is to properly account for the impact of the electrode potential on the interfacial energy landscape, which controls the kinetics of every electrochemical process. Most electronic structure methods, including DFT, are based on the canonical ensemble, where the number of particles remains unchanged.[16] Albeit, a system under control of the metal bulk phase potential can only be accurately described by a grand canonical ensemble where the number of electrons must be varied until a target chemical potential is attained.[17]

Computational approaches that have recently emerged strive to gain insight about the structure of the EDL that accounts for one or both of these factors.[11,16,18,19] One widely known methodology is the computational hydrogen electrode (CHE) of Rossmeisl and Nørskov.[20] The CHE has been used in studies of a plethora of phenomena taking place in the electrochemical interface,[20,21,22] such as the construction of surface Pourbaix diagrams,[23] water oxidation in cobalt oxides,[24] hydrogen oxidation and evolution reactions,[17] formation of the water bilayer near a Pt electrode under bias potential,[19] formation of reactive oxide species in Pt,[25] ethanol oxidation on a Pd electrode,[18] or CO_2 reduction on graphene-supported metal electrodes[26] and Ruthenium oxide catalysts.[27] In the CHE approach, the effect of the metal potential is treated by adding a fixed energy amount to each free electron in the reaction scheme that is proportional to the potential shift relative to equilibium.[20] This approach thus implies that the electronic structure of the solid phase can be determined under zero metal bulk phase potential, and the effect of the potential is only relevant when comparing different stationary points in the energy landscape. This assumption was continued to be applied when solvent contributions were added, whether explicitly or through a solvent model, as in studies of the graphene-supported electrochemical reduction of CO_2[28] or the effect of polarons on the overpotential of the oxygen evolution reaction.[29] The self-consistent energy calculation of the slab-solvent system is done under zero bias potential so the effects of the electrode potential on the ordering of the first layer of solvent molecules are not accounted for, which can lead to limitations in its application.[30]

For the case of the Pt surface in electrolyte solution, it is however well understood that strong correlations exist between charged surface state and the atomic configuration of near-surface solvent molecules.[16] In this case, coupling of the electronic structure of the metal electrode with electrode potential, pH, and adsorbate formation have to be taken into account self-consistently,

as a prerequisite for being able to extract relevant interface properties, such as the potential profile across the boundary region or the degree of ordering of the near-surface solvent layers.

While computational schemes with *a posteriori* corrections to pH or electrode potential, like the CHE, have had some success in studying the surface structure of metal electrodes away from the pzc, they offer no insights on other relevant properties in this region, such as the shape of the potential profile or the orientational susceptibility of the surface water layer. To provide such information, several methodologies have been developed, in which the effects of the medium and the metal bulk phase potential are considered during the electronic structure calculation.[31,32,33,34,35] One of such methods is the generalized computational hydrogen electrode (GCHE) that combines non-equilibrium Green's functions with DFT.[36] One of the most promising ones was published by Sundararaman *et al.*, in which the grand canonical free energy is minimized within the DFT scheme to reach a target chemical potential by fluctuating the number of electrons.[37] Recently, Otani *et al*.[38] developed a hybrid method, which considers the continuum solvent by modifying the reference interaction site method (RISM) of Hirata and Kovalenko,[39] from a 3D solvent model to an effective 1D model with solvent relaxation in the normal direction to the surface of the slab, treating the boundary region like a QM/MM system.[38] Similarly, the metal bulk phase potential is added by changing the periodic boundary condition (PBC) scheme of the solid state DFT framework, into a mixed boundary condition scheme where the normal direction is left open (i.e. not periodic). In the open direction, the Effective Screening Method (ESM) employs the Green function method in Laue representation to yield the electrostatic potential from an isolated slab.[38] The method, called ESM-RISM, can self-consistently account for the effects of solvent, pH, temperature and metal bulk phase potential. It has been employed to determine the reference hydrogen electrode potential,[40] and study lithium insertion/desorption processes in battery

materials.[41] However, as with other hybrid methods, most applications hitherto have been concerned with the potential region near the pzc, where adsorption effects are less important than further away from the pzc, and the interaction between metal surface and near solvent layers can be assumed – with reasonably accuracy – as being weak.[42]

In this work, we adopted the ESM-RISM method to study the charged Pt(111) surface in aqueous electrolyte solution, under conditions for the oxygen reduction reaction (ORR). The kinetics of the ORR are highly dependent on the structure of the interface,[42,43] which is determined by a multitude of parameters, including temperature, metal bulk phase potential, as well as ion concentration and pH in the solvent phase. Thus, it constitutes a good case study for the ESM-RISM description of interface properties in the potential region where the ORR takes place.

RESULTS AND DISCUSSION

Simulating metal bulk phase potential

The ESM-RISM hybrid method allows the modulation of the metal bulk phase potential, φ_M, either by adding a constant energy value to the chemical potential of electrons or by modifying the total number of electrons in the DFT system. In each case, the altered property is mirrored by the solvent system to preserve electroneutrality.[44] Consistent with the usual convention in electrochemical systems, the electrode potential is defined as the difference of φ_M to the solution phase potential, φ_S. Assuming for convenience and without loss of generality $\varphi_S = 0$, the electrode potential is therefore equal to φ_M.

In the particular case of the Pt-water system, an increasing electrode potential results in the formation of chemisorbed oxygen species at the Pt surface.[27,45,46] The oxide layer is of paramount importance when studying the electrochemical interface away from the pzc, as even qualitative

information on the potential-controlled interface phenomena is highly dependent on the effect of oxide layer formation on surface dipole moment and charge density, σ_M.[47]

In this work, a varying number of oxygen adatoms was added to the Pt surface in the DFT supercell, to reproduce the partial oxide coverage that corresponds to a given metal bulk phase potential. It must be remarked that the explicit addition of oxygen adatoms to the Pt surface is the only *ad hoc* aspect of the interface simulations in this work, since temperature, ion concentration (pH), water layer orientation, and metal work function are all treated self-consistently within the ESM-RISM framework.

The exact relation between metal bulk phase potential and surface charge is unknown beyond the qualitative non-monotonic behavior discovered by Frumkin and Petrii[48] and Garcia-Araez *et al*.[49] However, a mean field-type model of Huang *et al*.[50] provided an analytical solution for the charging relation that accounts for pH, temperature, water layer orientation and oxide coverage. In this work, we adopt this model to determine the normalized oxide coverage (θ_{OX}) that corresponds to each potential between the pzc and 1.0 V vs. SHE. Table 1 shows the oxide coverage and surface charge, as a function of the metal bulk phase potential (φ_M) according to the model of Huang *et al*.

Table 1. Normalized oxide coverage (θ_{OX}) and surface charge density (σ_M) as a function of metal phase potential φ_M, at pH 1 and 300 K according to the model of Huang *et al*.[50]

Slab label	# of O adatoms	φ_M (V)	θ_{OX}	σ_M (N_e/N_{Pt} x 10^{-3})
A	0	0.30	0.00	0.00
B	1	0.65	0.08	0.94
C	2	0.73	0.17	0.42
D	3	0.85	0.25	-1.95

E	4	0.90	0.33	-1.67
F	5	0.93	0.42	-1.51
G	6	0.96	0.50	-1.35
H	8	1.00	0.67	-1.14

We used the values presented in the above table to set the metal bulk phase potential for each slab. We chose to add this potential as a change in the total number of electrons rather than a Fermi level shift for two reasons: i) charge in the DFT model is distributed entirely on surface atoms and is mirrored by the first few solvent layers, in agreement with the experimental situation,[43] and ii) the shift in the Fermi level in the DFT model is not proportional to the metal phase potential.

Previous work by Otani *et al*. has shown that the ESM-RISM method can correctly determine metal bulk properties such as the work function as a function of the bulk electrolyte potential (φ_S) under a metal bulk phase electrode (or "metal phase") potential near the pzc.[38] In this region, the metal surface interacts weakly with near solvent molecules, and computational evidence suggests that water is disordered and displays the properties of bulk water.[15,51] However, other studies have shown that the presence of an oxide layer in the positive potential region imposes ordering of the first water layers, which shape the properties of the interface,[33,52] indicating a stronger interaction between the electrode and electrolyte phases than near the pzc.

The distance between the slab and the RISM region.

In the ESM-RISM framework, the DFT cell is positioned at a certain distance, *d*, in normal direction from the RISM region. To the best of our knowledge this parameter is empirical and, in a way, arbitrarily set, and apparently bears no impact on the free energy calculation. As shown in figure 1, the distance between the first water layer and the oxide-covered Pt surface remains largely unaffected by ***d*,** except at higher values of *d* (4 and 5 Å).

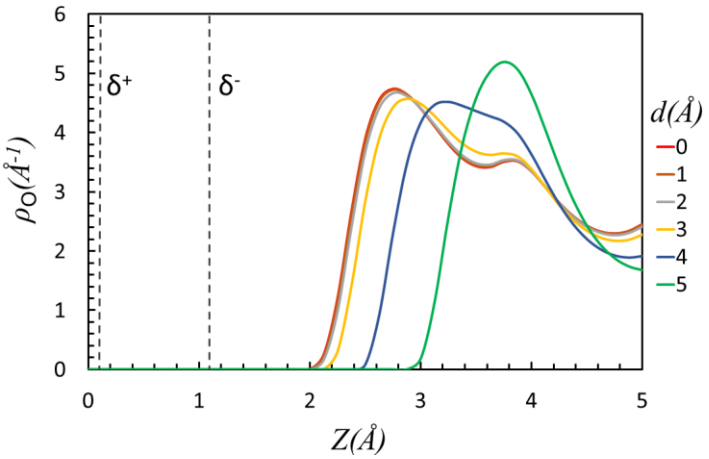

Figure 1. Plane-averaged linear density function of O atoms in H_2O solvent $\rho_O(r)$ (in [$Å^{-1}$]) in normal direction Z (in [Å]), obtained for different values of the parameter *d* that represents the distance between the DFT slab and the RISM region in the ESM-RISM code; *d* is varied from 0 to 5 Å. The dashed lines represent the position of the surface layer of Pt atoms (δ^+) and oxide layer (δ^-).

The function $\rho_o(r)$ reveals a modest impact of *d* on the position of the first water layer, defined by the distance of the first peak to the oxide layer (δ^-), which shifts from 1.7 Å at $d = 0$ to 2.8 Å at $d = 5$ Å. Bulk metal properties like the metal work function are not affected by *d*. The value of the work function for all values of *d* is 5.7 eV, with a variation of 0.02 V. Surface-dependent properties like the chemical potential of electrons μ_E, which corresponds to the Fermi energy in the ESM-RISM framework, are more sensitive to *d*. Figure 2 shows μ_E as a function of the metal phase potential φ_M for different values of d. In a similar fashion as $\rho_O(r)$ function, μ_E exhibits a mild variation, with *d* varying from 0 to 3 The variation is more pronounced at $d \geq 4$.

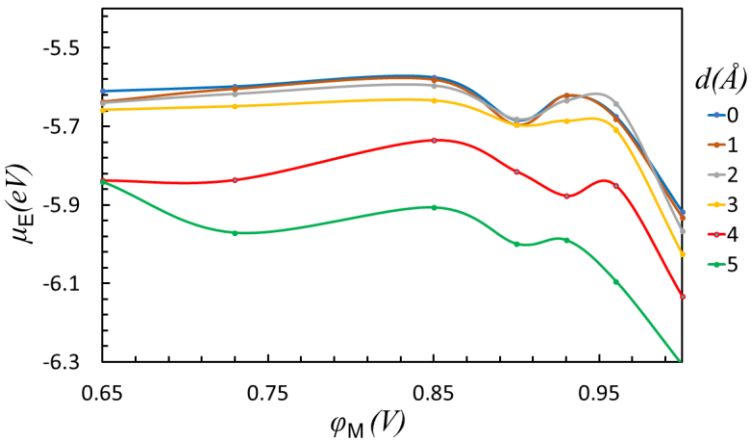

Figure 2. Chemical potential of electrons μ_E as a function of the metal phase potential φ_M for various values of d, as indicated in the legend.

In previous work by Otani *et al*.,[40] d was set to 5 Å to compute bulk properties like electrode and inner potential in weakly interacting systems, where interface effects have a smaller impact. Apparently, this value of d was chosen to model a solvated H_3O^+ molecule at 10 Å distance from the surface. To make the center of mass of all atoms locate around $Z = 0$, the slab was shifted to the left by 5 Å. In the case of the pristine slab calculation, the center of mass of the slab was placed at $Z = 0$. We would like to note that to the best of our knowledge the impact of d on interfacial properties has hitherto not been discussed in the framework of Otani *et al*.

Surface potential as a function of metal phase potential

The ORR is a reaction of utmost importance in electrochemical energy conversion. This reaction takes place at positive metal bulk phase potentials in the range of 0.8 to 1.0 V *vs*. SHE and, as has been shown, its kinetics are strongly influenced by properties such as oxide coverage and solvent layer orientation. Any theoretical approach that is used to study this reaction must correctly represent these properties at the potential of interest. In the case of ESM-RISM, this requires a qualitatively correct potential profile from the bulk of the metal to the bulk of the solution,

including regions in-between, to accurately capture the potential in the inner and outer Helmholtz planes. The structural model of Huang *et al*. contains an expression for the surface potential (outer Helmholtz potential φ_{OHP}) which is directly related to the surface charge. Since this potential depends on the position and orientation of the first few solvent layers, it constitutes a suitable property to assess the local potential profile derived from the ESM-RISM energy, in the frontier between the DFT and RISM regions.

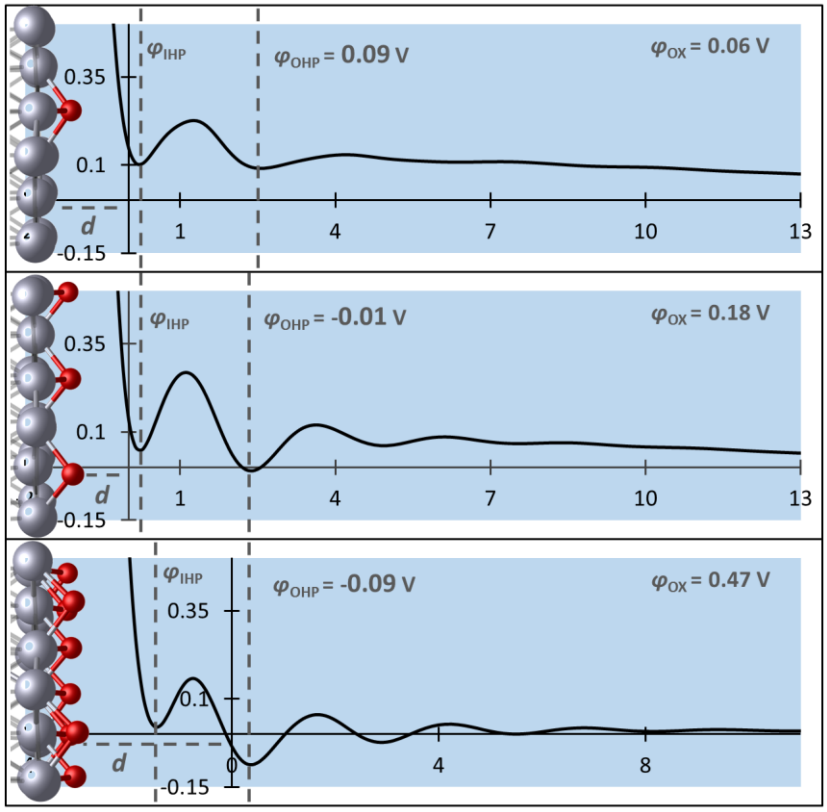

Figure 3. Plane-averaged local potential in V for slabs **B** (φ_M = 0.65 V), **D** (φ_M = 0.85 V), and **H** (φ_M = 1.00 V), with φ_{OHP} specified, and φ_{IHP} and *d* represented.

Figure 3 shows the local potential profile for three slabs at different surface charge values, with the value of φ_{OHP} as specified for each slab. φ_{OHP} is defined as the potential drop as a result of the accumulation of non-specifically adsorbed solvent and ion molecules near the surface, this property has the same non-monotonic character as the charging relation.[50] In the ESM-RISM

scheme, the first layer of adsorbed ions and water molecules is illustrated in figure 1 as the first density distribution peak (corresponding to the first inverted peak in figure 3), which constitutes the inner Helmholtz plane. The second solvent layer corresponds to the outer Helmholtz plane (second inverted peak in figure 3). Thus, φ_{OHP} was taken as the potential at the position of the second solvent and hydronium layer (in [V]), with the bulk solution potential as reference. For comparison with a monotonic property, the potential at the oxide layer (φ_{OX}) was obtained by subtracting the local potential energy of the oxide layer *in vacuo* from the local potential profiles presented in figure 3.

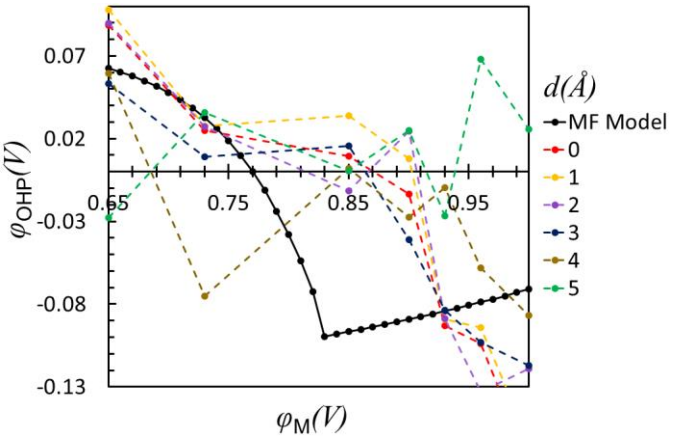

Figure 4. Surface potential φ_{OHP} as a function of metal phase potential φ_M (in [V]) compared to the mean field model by Huang *et al*. at each *d* value evaluated.

We have already established that the choice of *d* strongly affects intrinsic surface properties of the slab, such as μ_E, but ESM-RISM can still provide relative information, non-monotonic behavior remains unchanged regardless of *d*. This is not true when computing interface properties that are highly sensitive to the structure of the first solvent layers, such as φ_{OHP}. The potential profile near the surface is shaped by the position of the first solvent and ion layers, which are affected by *d*. As shown in figure 4, the downward trend in φ_{OHP} upon increasing φ_M, observed in the mean field model at potentials < 0.85 V vs. SHE, is not reproduced in the ESM-RISM model.

The trend in this function becomes highly irregular at higher values of d. Most notable, d = 5 Å results in positive φ_{OHP} at large φ_M, and d = 4 in negative φ_{OHP} at low φ_M.

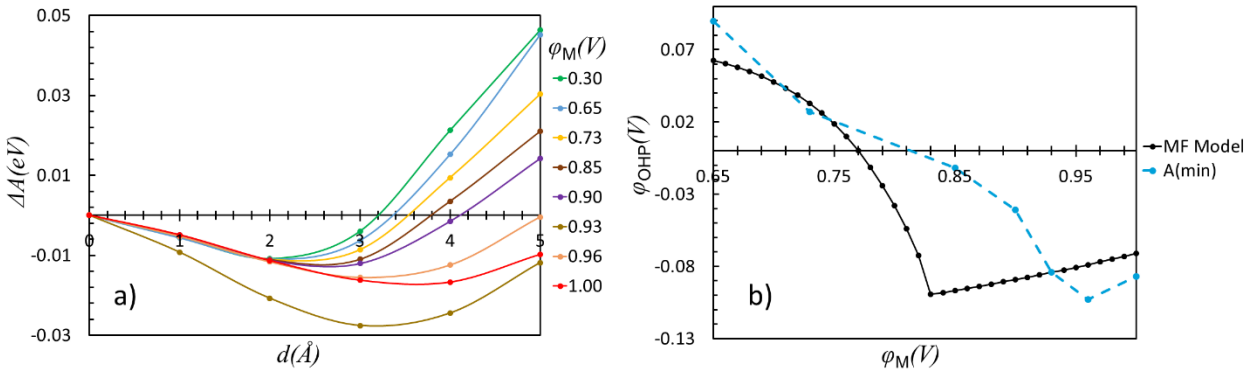

Figure 5. a) Free energy difference (ΔA) for each d value with d = 0 as reference point, in eV, for each φ_M sampled. b) Surface potential φ_{OHP} as a function of metal phase potential φ_M in V compared to the Mean Field model by Huang *et al*. at d with lowest free energy.

As previously shown, the choice of d affects the radial distribution function of the solvent and, as a result, the position of the near solvent layers. This in turn impacts the stabilization effect that each phase (solvent and electrode) has on the other, and thus the free energy of the system. Therefore, an energy optimization as a function of d can be carried out to find the optimal value of d for each configuration of the slab. Such an optimization would be internally consistent, since a lower free energy means the configuration is closer to thermodynamic equilibrium at that specific d.

Figure 5a shows the free energy of each slab at the d values sampled in this work with d = 0 as the reference value. The curves were obtained for only 6 values of d, so the lowest energy point, representing the optimal value of d, could be refined by sampling more points. However, the figure clearly shows that the optimal value of d varies with φ_M. In fact, there is a clear trend: the higher

the oxide coverage, the larger the optimal *d* value. Figure 5b shows φ_{OHP} vs φ_M this time using the "optimal" values of *d* obtained from the analysis of figure 5a. The plot exhibits much improved qualitative agreement with the mean field model, with the irregular variations being suppressed, suggesting that the φ_{OHP} description can be systematically improved by optimizing the value of *d* at any φ_M. Both mean field model and DFT/ESM-RISM approach calculate the relation between the surface charge density and the electrode potential self-consistently except for one *ad hoc* element, which is that the potential scale is pinned to the surface coverage with chemisorbed oxygen. Thus, the agreement between both approaches in the φ_{OHP} profile is an encouraging sign, in the sense that the physics underlying both approaches is essentially correct. As it stands, a manual optimization of *d* within the ESM-RISM implementation is impractical and would betray the self-consistency aim of the hybrid method. However, should an optimization method for *d* be implemented, it would greatly improve the applicability of ESM-RISM, especially in the computation of interface properties in highly interacting systems.

CONCLUSIONS

We have studied the oxidized Pt(111) surface in contact with a 0.1 M HCl electrolyte using the DFT/ESM-RISM hybrid method by Otani *et al*. In order to simulate an appropriate oxide coverage for a given value of the metal phase potential, we have used the model of Huang *et al*. We have assessed the viability of the computational method to study surface properties that are sensitive to the structure of the metal-solvent interface, such as chemical potential of electrons and surface potential. We found that the position of the metal slab with respect to the RISM solvent region, while having no clear physical meaning, has an impact on the optimization of the solvent and ion density profiles and correlation functions in proximity of the interface. This in turn affects the local potential profile in the surface region and energy levels of electrons as visible in the Fermi energy

shift. Moreover, a pronounced impact on the local potential drop in the first non-adsorbed solvent layer has been seen; the distance between the surface and the first solvent layer is influenced by the position of the metal slab, relative to the referential zero in the cell, and this effect is more apparent in the potential profile along the boundary region between solvent and electrode. This effect limits the applicability of DFT/ESM-RISM for studying electrochemical processes, specifically for reactions where the solvent plays an active role, as reactant, product or catalyst.

Finding a self-consistent method to describe the electrified interface is of paramount importance in electrocatalysis, and hybrid methods like DFT/ESM-RISM are at the frontier of that search. As previously shown by Otani *et al*., the method is competent when studying the electrified surface near or below the potential of zero charge, where solvent ordering is minimal and there is no specific adsorption. However, in order to gain meaningful information on the highly interacting situations like those favorable to the ORR, a more robust description of the ordering of solvent layers is needed. A good next step would be to include an optimization of the separation of the slab relative to the RISM region as part of the calculation. As it stands today, this is computationally unfeasible for most systems large enough to give meaningful DFT energies.

On a final note, we hope these insights can help improve existing hybrid methods and design new ones that can breach the gap between partial descriptions and fully self-consistent models. In particular, a robust hybrid method that can simulate surface properties of oxidized catalyst surfaces could be used in predictive calculations of novel materials that improve the atom economy of costly catalyst materials like Pt.

COMPUTATIONAL DETAILS

All DFT and ESM-RISM calculations were carried out using Quantum Espresso 6.1 version,[53] in the version modified by Otani *et al*.[38] The explicit atomic subsystem was described using the

exchange-correlation functional of Perdue-Burke-Ernzerhoff (PBE),[54],[55] with a plane-wave basis within the ultrasoft pseudopotential approximation. Cut-off energies were selected as 40 Ry for the wavefunction, and 320 Ry for the augmented charge. ESM-RISM calculations were performed in a vacuum/metal/solvent configuration to simulate the electrochemical interface between a Pt metal slab and a 0.1 M HCl solution (pH 1) at 300 K.

The modeled domain consisted of 4 layers of $2\sqrt{3}x2\sqrt{3}$ slabs of Pt(111), with converged k-point sampling of 4 x 4 x 1 centered on the Γ point. Occupation numbers were determined using a Gaussian smearing of 0,01 Ry broadening. The oxidized surface was prepared by adding O adatoms in the hollow positions of the slab. The number of adatoms varied from 1 to 8 for a range of coverages (θ_{OX}) between 1/12 and 2/3. The slabs were optimized in vacuum at the same DFT level of theory described above, and the optimized geometries were used in the ESM-RISM single-point calculations. The simulation cell dimensions were 9.77 x 9.77 Å in a 60^{o} angle, and the separation between the slab and the RISM region was sampled in a range from 0 to 5 Å. The RISM region was extended from 40 to 45 Å away from the slab.

The RISM region consisted of a H_2O solvent with a density of 1.00 g/mL at 300 K, and a 0.1 M electrolyte made up of H_3O^+ and Cl^- ions. The Laue-RISM open boundary calculation was performed using the Hirata and Kovalenko model for the closure,[39] and the RISM free energy was evaluated using the Gaussian fluctuation model with a cut-off energy of 160 Ry for the solvent distribution functions. Solvent correlation functions were converged with a tolerance of $1x10^{-6}$ Ry. The Lennard-Jones parameters of the electrode and adsorbate atoms in the classical force field calculations were σ_{Pt} = 2.65 Å and ε_{Pt} = 1.66 kcal mol^{-1} for Pt, and σ_O = 3.166 Å and ε_O = 0.1554 kcal mol^{-1} for O.[56]

Acknowledgements

We would like to acknowledge financial support of this work received under the Discovery Grants program of the Natural Sciences and Engineering Research Council of Canada (NSERC).

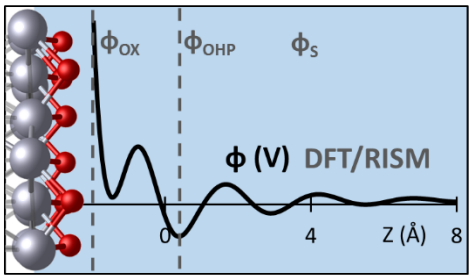

For Table of Contents Only (TOC Graphic)

---

[1] Lewis, N. S.; Nocera, D. G., Powering the Planet: Chemical Challenges in Solar Energy Utilization. *Proc. Natl. Acad. Sci. U.S.A.* **2006,** *103*, 15729.

[2] Bockris, J. O. M., Liquid Hydrogen. *Int. J. Hydrog. Energy* **2011,** *36*, 4617-4618.

[3] Simon, P.; Gogotsi, Y., Materials for Electrochemical Capacitors. *Nat. Mater.* **2008,** *7*, 845-854.

[4] Wang, Y.; Song, Y.; Xia, Y., Electrochemical Capacitors: Mechanism, Materials, Systems, Characterization and Applications. *Chem. Soc. Rev.* **2016,** *45*, 5925-5950.

[5] Magnussen, O. M., Ordered Anion Adlayers on Metal Electrode Surfaces. *Chem. Rev.* **2002,** *102*, 679-726.

[6] Bonnefont, A.; Ryabova, A. S.; Schott, T.; Kéranguéven, G.; Istomin, S. Y.; Antipov, E. V.; Savinova, E. R., Challenges in the Understanding Oxygen Reduction Electrocatalysis on Transition Metal Oxides. *Curr. Opin. Electrochem*. **2019,** *14*, 23-31.

[7] Huang, J.; Eikerling, M., Modeling the Oxygen Reduction Reaction at Platinum: A Brief Review of Recent Developments. *Curr. Opin. Electrochem* **2019**, *13*, 157-165.

[8] Poux, T.; Bonnefont, A.; Ryabova, A.; Kéranguéven, G.; Tsirlina, G. A.; Savinova, E. R., Electrocatalysis of Hydrogen Peroxide Reactions on Perovskite Oxides: Experiment *versus* Kinetic Modeling. *Phys. Chem. Chem. Phys.* **2014,** *16*, 13595-13600.

[9] Markiewicz, M.; Zalitis, C.; Kucernak, A., Performance Measurements and Modelling of the ORR on Fuel Cell Electrocatalysts – the Modified Double Trap Model. *Electrochim. Acta* **2015,** *179*, 126-136.

[10] van der Lee, A.; Roche, G. H.; Wantz, G.; Moreau, J. J. E.; Dautel, O. J.; Filhol, J.-S., Experimental and Theoretical Evidence of a Supercritical-like Transition in an Organic Semiconductor Presenting Colossal Uniaxial Negative Thermal Expansion. *Chem. Sci.* **2018,** *9*, 3948-3956.

[11] Calle-Vallejo, F.; Koper, M. T. M., First-principles Computational Electrochemistry: Achievements and Challenges. *Electrochim. Acta* **2012,** *84*, 3-11.

[12] Bai, M.; Cucinotta, C. S.; Jiang, Z.; Wang, H.; Wang, Y.; Rungger, I.; Sanvito, S.; Hou, S., Current-induced Phonon Renormalization in Molecular Junctions. *Phys. Rev. B* **2016,** *94*, 035411.

[13] Zhang, X.; Grabowski, B.; Körmann, F.; V Ruban, A.; Gong, Y.; C Reed, R.; Hickel, T.; Neugebauer, J., Temperature Dependence of the Stacking-fault Gibbs Energy for Al, Cu, and Ni. *Phys. Rev. B* **2018**, *98*, 224106-30.

[14] Clark, E. L.; Ringe, S.; Tang, M.; Walton, A.; Hahn, C.; Jaramillo, T. F.; Chan, K.; Bell, A. T., Influence of Atomic Surface Structure on the Activity of Ag for the Electrochemical Reduction of CO2 to CO. *ACS Catal.* **2019,** *9*, 4006-4014.

[15] Sakong, S.; Forster-Tonigold, K.; Groß, A., The Structure of Water at a Pt(111) Electrode and the Potential of Zero Charge Studied from First Principles. *J. Chem. Phys.* **2016,** *144*, 194701-194709.

[16] Eslamibidgoli, M. J.; Huang, J.; Kadyk, T.; Malek, A.; Eikerling, M., How Theory and Simulation can Drive Fuel Cell Electrocatalysis. *Nano Energy* **2016**, *29*, 334-361.

[17] Skúlason, E.; Tripkovic, V.; Björketun, M. E.; Gudmundsdóttir, S.; Karlberg, G.; Rossmeisl, J.; Bligaard, T.; Jónsson, H.; Nørskov, J. K., Modeling the Electrochemical Hydrogen Oxidation and Evolution Reactions on the Basis of Density Functional Theory Calculations. *J. Phys. Chem. C* **2010**, *114*, 18182-18197.

[18] Monyoncho, E. A.; Steinmann, S. N.; Michel, C.; Baranova, E. A.; Woo, T. K.; Sautet, P., Ethanol Electro-oxidation on Palladium Revisited Using Polarization Modulation Infrared Reflection Absorption Spectroscopy (PM-IRRAS) and Density Functional Theory (DFT): Why Is It Difficult To Break the C–C Bond? *ACS Catal.* **2016,** *6*, 4894-4906.

[19] Sakong, S.; Naderian, M.; Mathew, K.; Hennig, R. G.; Groß, A., Density Functional Theory Study of the Electrochemical Interface Between a Pt Electrode and an Aqueous Electrolyte using an Implicit Solvent Method. *J. Chem. Phys.* **2015,** *142*, 234107.

[20] Nørskov, J. K.; Rossmeisl, J.; Logadottir, A.; Lindqvist, L.; Kitchin, J. R.; Bligaard, T.; Jónsson, H., Origin of the Overpotential for Oxygen Reduction at a Fuel-Cell Cathode. *J. Phys. Chem. B* **2004,** *108*, 17886-17892.

[21] Eslamibidgoli, M. J.; Eikerling, M. H., Approaching the Self-consistency Challenge of Electrocatalysis with Theory and Computation. Current Opinion in Electrochemistry **2018**, *9*, 189-197.

[22] Seh, Z. W.; Kibsgaard, J.; Dickens, C. F.; Chorkendorff, I.; Nørskov, J. K.; Jaramillo, T. F., Combining Theory and Experiment in Electrocatalysis: Insights into Materials Design. *Science* **2017**, *355*, eaad4998.

[23] Hansen, H. A.; Rossmeisl, J.; Nørskov, J. K., Surface Pourbaix Diagrams and Oxygen Reduction Activity of Pt, Ag and Ni(111) Surfaces Studied by DFT. *Phys. Chem. Chem. Phys.* **2008**, *10*, 3722-3730.

[24] Bajdich, M.; García-Mota, M.; Vojvodic, A.; Nørskov, J. K.; Bell, A. T., Theoretical Investigation of the Activity of Cobalt Oxides for the Electrochemical Oxidation of Water. *J. Am. Chem. Soc.* **2013**, *135*, 13521-13530.

[25] Eslamibidgoli, M. J.; Eikerling, M. H., Electrochemical Formation of Reactive Oxygen Species at Pt (111)—A Density Functional Theory Study. *ACS Catal.* **2015**, *5*, 6090-6098.

[26] He, H.; Jagvaral, Y., Electrochemical Reduction of CO2 on Graphene Supported Transition Metals – Towards Single Atom Catalysts. *Phys. Chem. Chem. Phys.* **2017,** *19*, 11436-11446.

[27] Karamad, M.; Hansen, H. A.; Rossmeisl, J.; Nørskov, J. K., Mechanistic Pathway in the Electrochemical Reduction of CO2 on RuO2. *ACS Catal* **2015**, *5*, 4075-4081.

[28] He, H.; Morrissey, C.; Curtiss, L. A.; Zapol, P., Graphene-Supported Monometallic and Bimetallic Dimers for Electrochemical CO2 Reduction. *J. Phys. Chem. C* **2018,** *122*, 28629-28636.

[29] Gono, P.; Wiktor, J.; Ambrosio, F.; Pasquarello, A., Surface Polarons Reducing Overpotentials in the Oxygen Evolution Reaction. *ACS Catal.* **2018,** *8*, 5847-5851.

[30] Gauthier, J. A.; Ringe, S.; Dickens, C. F.; Garza, A. J.; Bell, A. T.; Head-Gordon, M.; Nørskov, J. K.; Chan, K., Challenges in Modeling Electrochemical Reaction Energetics with Polarizable Continuum Models. ACS Catalysis 2019, 9 (2), 920-931.

[31] Duan, Z.; Henkelman, G., Theoretical Resolution of the Exceptional Oxygen Reduction Activity of Au(100) in Alkaline Media. *ACS Catal.* **2019,** *9*, 5567-5573.

[32] Hörmann, N. G.; Andreussi, O.; Marzari, N., Grand Canonical Simulations of Electrochemical Interfaces in Implicit Solvation Models. *J. Chem. Phys.* **2019,** *150*, 041730.

[33] Alfonso, D. R.; Tafen, D. N.; Kauffmann, D. R., First-Principles Modeling in Heterogeneous Electrocatalysis. *Catalysts* **2018,** *8*, 424.

[34] Petrosyan, S. A.; Rigos, A. A.; Arias, T. A., Joint Density-Functional Theory: Ab Initio Study of Cr2O3 Surface Chemistry in Solution. *J. Phys. Chem. B* **2005,** *109*, 15436-15444.

[35] Joseph, G.; Colin, D.; Hendrik H., H.; Stefan, R.; Karen, C., Unified Approach to Implicit and Explicit Solvent Simulations of Electrochemical Reaction Energetics. 2019.

[36] Hansen, M. H.; Jin, C.; Thygesen, K. S.; Rossmeisl, J., Finite Bias Calculations to Model Interface Dipoles in Electrochemical Cells at the Atomic Scale. *J. Phys. Chem. C* **2016**, *120*, 13485-13491.

[37] Sundararaman, R.; Goddard III, W. A.; Arias, T. A., Grand Canonical Electronic Density-Functional Theory: Algorithms and Applications to Electrochemistry. *J. Chem. Phys.* **2017,** *146*, 114104.

[38] Nishihara, S.; Otani, M., Hybrid Solvation Models for Bulk, Interface, and Membrane: Reference Interaction Site Methods Coupled with Density Functional Theory. *Phys. Rev. B* **2017,** *96*, 115429.

[39] Kovalenko, A.; Hirata, F., Self-Consistent Description of a Metal–Water Interface by the Kohn–Sham Density Functional Theory and the Three-Dimensional Reference Interaction Site Model. *J. Chem. Phys.* **1999,** *110*, 10095-10112.

[40] Haruyama, J.; Ikeshoji, T.; Otani, M., Electrode Potential from Density Functional Theory Calculations Combined with Implicit Solvation Theory. *Phys. Rev. Mater.* **2018,** *2*, 095801.

[41] Haruyama, J.; Ikeshoji, T.; Otani, M., Analysis of Lithium Insertion/Desorption Reaction at Interfaces between Graphite Electrodes and Electrolyte Solution Using Density Functional + Implicit Solvation Theory. *J. Phys. Chem. C* **2018,** *122*, 9804-9810.

[42] Rinaldo, S. G.; Stumper, J.; Eikerling, M., Physical Theory of Platinum Nanoparticle Dissolution in Polymer Electrolyte Fuel Cells. *J. Phys. Chem. C* **2010,** *114*, 5773-5785.

[43] Briega-Martos, V.; Herrero, E.; Feliu, J. M., Effect of pH and Water Structure on the Oxygen Reduction Reaction on platinum electrodes. *Electrochim. Acta* **2017**; *241*, 497-509.

[44] Otani, M.; Hamada, I.; Sugino, O.; Morikawa, Y.; Okamoto, Y.; Ikeshoji, T., Electrode Dynamics from First Principles. *J. Phys. Soc. Jpn.* **2008,** *77*, 024802.

[45] Rinaldo, S. G.; Lee, W.; Stumper, J.; Eikerling, M., Nonmonotonic Dynamics in Lifshitz-Slyozov-Wagner Theory: Ostwald Ripening in Nanoparticle Catalysts. *Phys. Rev. E* **2012,** *86*, 041601.

[46] Rinaldo, S. G.; Lee, W.; Stumper, J.; Eikerling, M., Mechanistic Principles of Platinum Oxide Formation and Reduction, *Electrocatalysis*, **2014**, *5*, 262-272

[47] Jinnouchi, R.; Anderson, A. B., Electronic Structure Calculations of Liquid-Solid Interfaces: Combination of Density Functional Theory and Modified Poisson-Boltzmann Theory. *Phys. Rev. B* **2008,** *77*, 245417.

[48] Frumkin, A. N.; Petrii, O. A., Potentials of Zero Total and Zero Free Charge of Platinum Group Metals. *Electrochim. Acta* **1975,** *20*, 347-359.

[49] Garcia-Araez, N.; Climent, V.; Feliu, J., Potential-Dependent Water Orientation on Pt(111), Pt(100), and Pt(110), As Inferred from Laser-Pulsed Experiments. Electrostatic and Chemical Effects. *J. Phys. Chem. C* **2009,** *113*, 9290-9304.

[50] Huang, J.; Zhang, J.; Eikerling, M., Unifying Theoretical Framework for Deciphering the Oxygen Reduction Reaction on Platinum. *Phys. Chem. Chem. Phys.* **2018,** *20*, 11776-11786.

[51] Schnur, S.; Groß, A., Properties of Metal–Water Interfaces Studied from First Principles. *New J. Phys.* **2009,** *11*, 125003.

[52] Taylor, C. D.; Neurock, M., Theoretical Insights into the Structure and Reactivity of the Aqueous/Metal Interface. *Curr. Opin. Solid St. M.* **2005,** *9*, 49-65.

[53] Giannozzi, P.; Baroni, S.; Bonini, N.; Calandra, M.; Car, R.; Cavazzoni, C.; Ceresoli, D.; Chiarotti, G. L.; Cococcioni, M.; Dabo, I.; Dal Corso, A.; de Gironcoli, S.; Fabris, S.; Fratesi, G.;

Gebauer, R.; Gerstmann, U.; Gougoussis, C.; Kokalj, A.; Lazzeri, M.; Martin-Samos, L.; Marzari, N.; Mauri, F.; Mazzarello, R.; Paolini, S.; Pasquarello, A.; Paulatto, L.; Sbraccia, C.; Scandolo, S.; Sclauzero, G.; Seitsonen, A. P.; Smogunov, A.; Umari, P.; Wentzcovitch, R. M., QUANTUM ESPRESSO: a Modular and Open-Source Software Project for Quantum Simulations of Materials. *J. Phys. Condens. Matter* **2009,** *21*, 395502.

[54] Perdew, J. P.; Burke, K.; Ernzerhof, M., Generalized Gradient Approximation Made Simple Erratum *Phys. Rev. Lett.* **1997,** *78*, 1396-1396.

[55] Perdew, J. P.; Burke, K.; Ernzerhof, M., Generalized Gradient Approximation Made Simple. *Phys. Rev. Lett.* **1996,** *77*, 3865-3868.

[56] Rappe, A. K.; Casewit, C. J.; Colwell, K. S.; Goddard, W. A.; Skiff, W. M., UFF, a Full Periodic Table Force Field for Molecular Mechanics and Molecular Dynamics Simulations. *J. Am. Chem. Soc.* **1992,** *114*, 10024-10035.